Journal of Visualized Experiments

Quantitative SERS Detection of Uric Acid via Formation of Precise Plasmonic Nanojunctions within Aggregates of Gold Nanoparticles and Cucurbit[n]uril

--Manuscript Draft--

Article Type:	Invited Methods Article - JoVE Produced Video
Manuscript Number:	JoVE61682R2
Full Title:	Quantitative SERS Detection of Uric Acid via Formation of Precise Plasmonic Nanojunctions within Aggregates of Gold Nanoparticles and Cucurbit[n]uril
Corresponding Author:	Tung-Chun Lee University College London London, London UNITED KINGDOM
Corresponding Author's Institution:	University College London
Corresponding Author E-Mail:	tungchun.lee@ucl.ac.uk
Order of Authors:	Weng-I Katherine Chio
	Gemma Davison
	Tabitha Jones
	Jia Liu
	Ivan P. Parkin
	Tung-Chun Lee
Additional Information:	
Question	**Response**
Please indicate whether this article will be Standard Access or Open Access.	Standard Access (US$2,400)
Please indicate the **city, state/province, and country** where this article will be **filmed**. Please do not use abbreviations.	London, United Kingdom
Please confirm that you have read and agree to the terms and conditions of the author license agreement that applies below:	I agree to the UK Author License Agreement (for UK authors only)
Please specify the section of the submitted manuscript.	Chemistry
Please provide any comments to the journal here.	

TITLE:

Quantitative SERS Detection of Uric Acid via Formation of Precise Plasmonic Nanojunctions within Aggregates of Gold Nanoparticles and Cucurbit[*n*]uril

AUTHORS AND AFFILIATIONS:

Weng-I Katherine Chio[1], Gemma Davison[1], Tabitha Jones[1], Jia Liu[1], Ivan P. Parkin[1], Tung-Chun Lee[1,2,*]

[1]Department of Chemistry, University College London (UCL), London, U.K.
[2]Institute for Materials Discovery, University College London (UCL), London, U.K.

Email address of co-authors:

Weng-I Katherine Chio	(weng.chio.16@ucl.ac.uk)
Gemma Davison	(gemma.davison.18@ucl.ac.uk)
Tabitha Jones	(tabitha.jones.19@ucl.ac.uk)
Jia Liu	(ucqsjli@ucl.ac.uk)
Ivan P. Parkin	(i.p.parkin@ucl.ac.uk)

*Corresponding author:

Tung-Chun Lee	(tungchun.lee@ucl.ac.uk)

KEYWORDS:

Gold nanoparticles, automated synthesizer, cucurbit[*n*]uril, host-guest complexation, self-assembly, surface-enhanced Raman spectroscopy, sensor, biomarkers, diseases diagnosis

SUMMARY:

A host-guest complex of cucurbit[7]uril and uric acid was formed in an aqueous solution before adding a small amount into Au NP solution for quantitative surface-enhanced Raman spectroscopy (SERS) sensing using a modular spectrometer.

ABSTRACT:

This work describes a rapid and highly sensitive method for the quantitative detection of an important biomarker, uric acid (UA), via surface-enhanced Raman spectroscopy (SERS) with a low detection limit of ~0.2 μM for multiple characteristic peaks in the fingerprint region, using a modular spectrometer. This biosensing scheme is mediated by the host-guest complexation between a macrocycle, cucurbit[7]uril (CB7), and UA, and the subsequent formation of precise plasmonic nanojunctions within the self-assembled Au NP: CB7 nanoaggregates. A facile Au NP synthesis of desirable sizes for SERS substrates has also been performed based on the classical citrate-reduction approach with an option to be facilitated using a lab-built automated synthesizer. This protocol can be readily extended to multiplexed detection of biomarkers in body fluids for clinical applications.

INTRODUCTION:

Uric acid, which is the end product of metabolism of purine nucleotides, is an important

biomarker in blood serum and urine for the diagnosis of diseases such as gout, preeclampsia, renal diseases, hypertension, cardiovascular diseases and diabetes[1-5]. Current methods for uric acid detection include colorimetric enzymatic assays, high performance liquid chromatography and capillary electrophoresis, which are time-consuming, expensive and require sophisticated sample preparation[6-9].

Surface-enhanced Raman spectroscopy is a promising technique for routine point-of-care diagnosis as it allows selective detection of biomolecules via their vibration fingerprints and offers numerous advantages such as high-sensitivity, rapid response, ease of use and no or minimal sample preparation. SERS substrates based on noble metal nanoparticles (e.g., Au NPs) can enhance the Raman signals of the analyte molecules by 4 to 10 orders of magnitude[10] via strong electromagnetic enhancement caused by surface plasmon resonance[11]. Au NPs of tailored sizes can be easily synthesized as opposed to the time-consuming fabrication of complex metal nanocomposites[12], and thus are widely used in biomedical applications owing to their superior properties[13-16]. Attachment of macrocyclic molecules, cucurbit[*n*]urils (CB*n*, where *n* = 5-8, 10), onto the surface of Au NPs can further enhance the SERS signals of the analyte molecules as the highly symmetric and rigid CB molecules can control the precise spacing between the Au NPs and localize the analyte molecules at the center or in close proximity to the plasmonic hotspots via formation of host-guest complexes (**Figure 1**)[17-20]. Previous examples of SERS studies using Au NP: CB*n* nanoaggregates include nitroexplosives, polycyclic aromatics, diaminostilbene, neurotransmitters and creatinine[21-25], with the SERS measurements either being performed in a cuvette or by loading a small droplet onto a custom-made sample holder. This detection scheme is particularly useful to rapidly quantify biomarkers in a complex matrix with a high reproducibility.

Herein, a facile method to form host-guest complexes of CB7 and an important biomarker UA, and to quantify UA with a detection limit of 0.2 μM via CB7-mediated aggregations of Au NPs in aqueous media was demonstrated using a modular spectrometer, which is promising for diagnostic and clinical applications.

PROTOCOL:

1. Synthesis of Au NPs

1.1. Synthesis of Au seeds via the conventional Turkevich method[26]

1.1.1. Prepare 10 mL of 25 mM $HAuCl_4$ solution by dissolving 98.5 mg of $HAuCl_4 \cdot 3H_2O$ precursor with 10 mL of deionized water in a glass vial.

NOTE: Transfer a small amount of $HAuCl_4$ precursor into a weighing boat and use a plastic spatula instead of metallic spatula to weigh out the crystals because $HAuCl_4$ precursor will corrode metal labware. The weighing step should be performed as swiftly as possible, since $HAuCl_4$ is hygroscopic and will therefore increase its weight over time by absorbing water from the atmosphere. $HAuCl_4$ is highly corrosive and can cause severe skin burns and eye damage.

Take extra care when handling it.

1.1.2. Prepare 0.5 mL of 500 mM sodium citrate solution by dissolving 64.5 mg of sodium citrate powder with 0.5 mL of deionized water in a glass vial.

1.1.3. Dilute 1 mL of the 25 mM $HAuCl_4$ solution with 99 mL water in a 250 mL blue-capped bottle to give 100 mL of 0.25 mM $HAuCl_4$ solution.

1.1.4. Add 99.5 mL of the 0.25 mM $HAuCl_4$ solution into a 250 mL three-necked round-bottomed flask equipped with a condenser. Heat the solution to 90 °C under vigorous stirring and maintain the temperature for 15 min.

1.1.5. Inject 0.5 mL of the 500 mM sodium citrate solution into the reaction mixture and maintain the temperature and stirring until the color of the solution turns ruby-red.

NOTE: The reaction takes about 30 min.

1.2. Seeded growth of Au NPs via the kinetically-controlled method[13]

1.2.1. Cool the as-synthesized Au seed solution to 70 °C.

1.2.2. Prepare 10 mL of 60 mM sodium citrate solution by dissolving 154.8 mg of sodium citrate powder with 10 mL of deionized water in a glass vial.

1.2.3. Inject 0.67 mL of the 25 mM $HAuCl_4$ solution and 0.67 mL of the 60 mM sodium citrate solution to the Au seeds with a time interval of 2 min.

1.2.4. Repeat step 1.2.3 to gradually increase the size of Au NPs to 40 nm.

NOTE: It takes about 10 growing steps to reach 40 nm. The actual number of steps needed may be dependent on the precise set-up.

1.3. Seeded growth of Au NPs using automated synthesizer (Figure 2)

1.3.1. Transfer 25 mL of the Au seed solution prepared in section 1 to a 50 mL conical centrifuge tube and cool to 70 °C in a thermomixer.

NOTE: Monitor the temperature inside the thermomixer using a thermocouple thermometer placed in a 50 mL centrifuge tube containing 25 mL of water.

1.3.2. Fill a 3 mL Luer lock disposable syringe with 2.5 mL of 25 mM $HAuCl_4$ solution. Fill another 3 mL Luer lock disposable syringe with 2.5 mL of 60 mM sodium citrate solution.

1.3.3. Place the syringes in the syringe pumps and use Luer-to-MicroTight adapters to connect

the PEEK tubing (150 µm internal diameter) to the syringes. Insert the tubing into the centrifuge tube containing the Au seed solution in the thermomixer.

1.3.4. Set both syringe pumps to dispense 0.1675 mL of solution over 20 min (8.357 µL per min).

1.3.5. Set the thermomixer rotation speed to 700 rpm and press **Start** on the syringe pump containing the 25 mM $HAuCl_4$ solution.

1.3.6. After 2 min, press **Start** on the syringe pump containing the 60 mM sodium citrate solution.

1.3.7. 30 min after starting the $HAuCl_4$ solution injection, remove an aliquot of the Au NP solution for analysis.

1.3.8. Repeat steps 1.3.5 – 1.3.7 to gradually increase the diameter of the Au NPs up to 40 nm.

NOTE: This setup can be used to grow Au NPs up to 40 nm in one step by increasing the volume of reactants added in step 1.3.4. This is achieved by increasing the dispensing time whilst maintaining the same rate of injection.

2. Characterization of Au NPs

2.1. UV-Vis spectroscopy

2.1.1. Add 1 mL of the Au NP solution to a semi-micro quartz cuvette.

2.1.2. Turn on the spectrometer.

2.1.3. Set the wavelength range to 400 - 800 nm.

2.1.4. Acquire the UV-Vis spectrum for each sample.

2.2. Dynamic light scattering (DLS)

2.2.1. Filter the sample solution into a plastic semi-micro cuvette with a 0.22 µm filter.

2.2.2. Turn on the DLS instrument.

2.2.3. Set the temperature to 25 °C and equilibrate for 60 s.

2.2.4. Measure the hydrodynamic size of each sample.

2.3. Transmission electron microscopy (TEM)

2.3.1. Drop-cast a 5 µL droplet of the sample solution onto a C-coated 300-mesh Cu grid and dry in air.

NOTE: Dilution is needed for more concentrated Au NP solution samples to obtain well dispersed Au NPs on a TEM grid.

2.3.2. Acquire multiple TEM images for each sample using a TEM at 200 kV acceleration voltage.

2.3.3. Measure the diameter of 200 Au NPs for each sample using ImageJ to calculate the average size and standard deviation.

3. Formation of CB7-UA complexes

3.1. Preparation of 0.4 mM CB7 solution

3.1.1. Add 4.65 mg of CB7 to a 15 mL glass vial.

NOTE: The amount of CB7 is calculated based on the formula weight of CB7 (= 1163 Da) which has been employed by most reports in the literature. Nevertheless, CB7 solid samples typically contain water, HCl, methanol and other salts left from the synthesis and purification steps, contributing to ~10 – 20% dead weight in the sample. The trapped solvents and salts could not be removed by heating in a vacuum oven or other means. Their amounts vary between different batches of samples but can be quantified using elemental analysis. Yet, the presented protocol is not sensitive to the presence of unquantified amount of solvents and salts in the CB7 samples.

3.1.2. Add 10 mL of water to the vial and tighten the cap.

3.1.3. Sonicate the sample at room temperature until the CB7 solid is completely dissolved.

NOTE: CB7 was synthesized according to literature[27] but it is also commercially available.

3.2. Preparation of 0.4 mM UA solution

3.2.1. Add 2.69 mg of UA to a 50 mL centrifuge tube.

3.2.2. Add 40 mL of water to the tube and tighten the cap.

3.2.3. Use a thermomixer to swirl the sample solution by setting the temperature to 70 °C, speed to 800 rpm and time to 2 h. Allow the solution to cool to room temperature.

NOTE: UA has a low solubility in water (0.40 mM)[5]. Swirl for longer if the UA powder has not

been dissolved completely. Alternatively, ultrasonication can be used to facilitate the dissolution.

3.3. Sequential dilutions of the 0.4 mM UA solution

3.3.1. Dilute 5 mL of the 0.4 mM UA solution with 5 mL water in a 15 mL glass vial to give 10 mL of 0.2 mM UA solution. Tighten the cap and sonicate for 30 s.

3.3.2. Repeat step 3.3.1 using an appropriate amount of UA and water as described in Table 1.

3.4. Preparation of the CB7-UA complexes

3.4.1. Add 0.75 mL of the 0.4 mM CB7 solution and 0.75 mL of 0.4 mM UA solution into a 1.5 mL tube. Secure the lid and sonicate for 30 s.

3.4.2. Wait for 30 min to ensure the formation of host-guest complexes.

3.4.3. Repeat step 3.4.1 – 3.4.2 using UA solution of different concentrations.

4. SERS sensing of UA

4.1. Experimental set-up of the Raman system (**Figure 3**)

4.1.1. Switch on the 633 nm He-Ne laser (22.5 mW).

4.1.2. Switch on the modular Raman spectrometer.

4.1.3. Switch on the computer and start the software.

4.1.4. Click the **Spectroscopy Application Wizards** Icon, and then select **Raman**.

4.1.5. Start a new acquisition. Set the integration time to 30 s, scans to average to 5 and boxcar to 0.

4.1.6. Store background spectrum and enter the laser wavelength (i.e., 633 nm).

NOTE: Integration time is the time for each scan, scans to average is number of scans averaged to create each spectrum and boxcar is the number of neighboring pixels averaged[28].

4.2. Formation of the SERS substrates

4.2.1. Add 0.9 mL of the 40 nm Au NP solution and 0.1 mL of the pre-formed CB7-UA complex solution into a 1.5 mL tube. Secure the lid and sonicate until the solution changes from ruby-red to purple.

NOTE: Commercial citrate-stabilized 40 nm Au NP solution samples can also be used. Typically, the optical density of the localized surface plasmon resonance (LSPR) peak is adjusted to 1 via dilution from concentrated stock solution samples. Citrate concentration in the sample is typically kept as 2 mM.

4.2.2. Transfer the sample solution to a semi-micro cuvette. Place the cuvette into the Raman sample holder and close the cover.

4.2.3. Start the measurement.

4.2.4. Set up the auto-saving to record five consecutive SERS spectra.

4.2.5. Stop the measurement and change the sample.

4.2.6. Repeat step 4.2.1 – 4.2.5 using CB7-UA solution of different concentrations.

NOTE: Aggregation time is found to be dependent on the concentration of UA in the nanoaggregates, ranging from 30 s for 0.1 μM UA to 30 min for 20 μM UA, owing to the difference in the concentration of empty CB7 which has major contribution to mediating the aggregation of Au NPs. For the CB7-UA complex, one portal is blocked by the bulky UA molecule, rendering it unavailable for binding to the Au NP surface and therefore unable to mediate the NP aggregation[21]. The sample is ready for measurement when the color of the solution changes from ruby-red to purple.

5. Data analysis

5.1. Data processing

5.1.1. Download and install the baseline with asymmetric least squares (ALS) plugin into Origin.

NOTE: The ALS plugin requires OriginPro.

5.1.2. Insert the raw data into Origin.

5.1.3. Calculate an average value from the five SERS spectra of each sample. Divide the value by the power of the laser (i.e., 22.5 mW) and by the integration time (i.e., 30 s).

5.1.4. Click the **ALS** icon to open the dialog. Set the asymmetric factor to 0.001, threshold to 0.03 %, smoothing factor to 2 and number of iterations to 20 to correct the baseline of each averaged spectrum.

5.1.5. Plot the SERS spectra of different UA concentrations using stacked lines by y offsets. The

output should be intensity (counts s^{-1} mW^{-1}) against Raman shift (cm^{-1}).

REPRESENTATIVE RESULTS:

In the presented Au NP synthesis, the UV-Vis spectra show a shift of the LSPR peaks from 521 nm to 529 nm after 10 growing steps (**Figure 4A,B**) while the DLS data shows a narrow size distribution as the size of Au NPs increase from 25.9 nm to 42.8 nm (**Figure 4C,D**). The average sizes of G0, G5 and G10 measured from TEM images (**Figure 4E**) are 20.1 ± 2.1 nm, 32.5 ± 2.3 nm and 40.0 ± 2.2 nm respectively, with 200 particles counted in each case. These results indicate this protocol is effective in synthesizing uniform and narrowly dispersed Au NPs.

In the presented SERS studies, host-guest complexes of CB7 and UA were formed with empty CB7 mediating the formation of precise plasmonic nanojunctions within the Au NP: CB7 nanoaggregates, as supported by the characteristic UA signals in the SERS spectrum (**Figure 5A**). The assignments for the Raman peaks of CB (marked by +) and UA (marked by *) are shown in **Table 2**. Conversely, no SERS signals of UA can be observed in the absence of CB7, illustrating the key role of CB7 in triggering the aggregation of Au NPs.

A constant CB7 concentration of 20 μM was used in the SERS titration of UA throughout so as to ensure the in situ formation of reproducible plasmonic nanostructures (i.e., SERS substrates). The high sensitivity of the detection scheme presented in this protocol was demonstrated by the observation of clear SERS signals from the UA peaks at 640 cm^{-1} and 1130 cm^{-1} (attributed to skeletal ring deformation and C-N vibration respectively) down to ~0.2 μM (**Figure 5B–D**), which is known as the detection limit. In addition, very strong correlations (R^2 > 0.98) between the SERS intensity and log concentration of UA were obtained by power law for both peaks, with linear regions found in the range of 0.2 to 2 μM (**Figure 5E,F**). It should be noted that linear correlations between the SERS intensity and log concentration can be approximated for a narrow range of analyte concentrations, whereas the SERS signal approaches 0 when the log concentration approaches negative infinity (i.e., the analyte concentration approaches 0), as observed in our data. The SERS signals are also highly reproducible as evidenced by the small error bars shown in **Figure 5E,F**.

FIGURE AND TABLE LEGENDS:

Figure 1: Schematic illustration of the precise plasmonic nanojunctions within self-assembled Au NP: CB7 nanoaggregates. Inset shows a zoom-in of the plasmonic nanojunctions where the aggregation is mediated by empty CB7 while UA is enriched on the surface of Au NPs via host-guest complexation. It is noted that the scheme is not drawn to scale.

Figure 2: (a) Schematic illustration and (b) photograph of the automated Au NP synthesizer.

Figure 3: Schematic illustration of the Raman system.

Figure 4: Representative characterization of Au NPs. (**A**) UV-Vis spectra of Au NPs and (**B**) zoom-in spectra showing the shifting of the LSPR peaks as the number of growing steps increases to 10. (**C**) Hydrodynamic size of Au NPs and (**D**) corresponding plot of particle size as a

function of number of growing steps. (**E**) TEM images of Au NPs, showing sizes of Au seeds and Au NPs after 5 and 10 growing steps.

Figure 5: Representative SERS results of UA detection within Au NP: CB7 nanoaggregates. (A) SERS spectra of UA in the presence or absence of CB7. Raman peaks of CB7 and UA are marked by + and * respectively. (B) Full-range, (C) 600 - 700 cm^{-1} zoom-in and (D) 1100 - 1180 cm^{-1} zoom-in SERS spectra of UA with concentrations from 0 to 20 μM. Main Raman peaks of UA are marked by *. Spectra were baseline corrected and offset for clarity. (E,F) Corresponding plots of the SERS peak intensity against concentration of UA.

Table 1: Sequential dilutions of UA solution.

Table 2: Assignments for the Raman peaks of CB7 and UA[2,4,29].

DISCUSSION:

The automated synthesis method described in the protocol allows Au NPs of increasing sizes to be reproducibly synthesized. Although there are some elements that still need to be carried out manually, such as the fast addition of sodium citrate during the seed synthesis and checking periodically to ensure that the PEEK tubing is secure, this method allows Au NPs of large sizes (up to 40 nm), which would usually require multiple manual injections of $HAuCl_4$ and sodium citrate, to be synthesized via continuous addition over a long period of time.

Further characterization can be performed to elucidate the fundamental property of the CB complexes. For instance, the formation of host-guest complexes can typically be confirmed using ^1H nuclear magnetic resonance (NMR), which should show upfield shift and broadening of signals in case of complexation[21,22,25]. Yet ^1H NMR is not applicable to UA due to its lack of non-exchangeable protons. Alternative techniques such as ^{13}C NMR and mass spectrometry could also be employed to characterize the complexation. Binding constants between CB7 and UA can be measured using titration techniques, such as UV-Vis spectroscopy titration and isothermal titration calorimetry (ITC)[21,22,25]. Meanwhile molecular modelling based on force-field and density functional theory (DFT) models can be computed to obtain theoretical insights into the binding geometry of the host-guest complexes[21,22,25,29]. Moreover IR and Raman spectra can be computed by frequencies calculations[21,25,29].

SERS is a highly sensitive and selective analytical technique which allows identification of trace analytes via their molecule-specific vibrational fingerprints. SERS is gaining interests across different science disciplines, in particular biomedical studies, due to its greatly enhanced signals, much shorter acquisition time and high tolerance to liquid water (suitable for sensing in biofluids)[30-35]. In contrast to previous reports on UA sensing[1-4,36,37], the rigid structure of CB7 defines precise spacing of 0.9 nm between Au NPs via carbonyl portal binding while the surface-bound CB7 can trap UA molecules within its cavity (**Figure 1**), resulting in strong and localized plasmonic hotspots, and hence the highly sensitive (down to ~0.2 μM) and reproducible (within 2% error) SERS signals of UA with very strong correlations ($R^2 > 0.98$) between the SERS intensity and log concentration (**Figure 5**).

In an attempt to optimize the concentration of CB7, we note that 20 µM CB7 was used to ensure the formation of reproducible SERS substrates. In particular, the absolute concentration of CB7 used is dependent on the overall system (i.e., Au NPs, analytes and background molecules, if any)[18,22]. A higher concentration of CB7 should be used if the aggregation of Au NPs is too slow. Conversely, a lower concentration of CB7 should be used if the sample solution precipitates quickly and leads to shorter measurement windows. The aggregation of Au NPs mediated by CB7 in our experimental setting is expected to follow the diffusion-limited colloidal aggregation (DLCA) kinetics[19], in which open and elongated chain-like structures were rapidly formed initially before joining together as quasi-fractal network. DLCA kinetics typically occurs at a high CB: Au NP ratio (by number), which is equal to 10^6:1 in our case. It should be noted that uric acid is present in bodily fluids (e.g., blood serum, urine) at a higher concentration. For instance, the normal concentration of uric acid is 3.5 – 7.0 mg/dL in blood serum[38] and 16 – 100 mg/dL in urine[2] respectively (concentration above or below the normal concentration is known as hyperuricemia and hypouricemia)[39]. Therefore, only a very small amount of sample is needed for biomarker detection in this highly sensitive scheme where a high dilution factor is used to lower the concentration of the sample to a suitable range. This is particularly important for point-of-care monitoring of terminally ill patients whose urine excretion is very low. Highly diluted samples result in larger sample volumes and thus reduce errors in the quantification of biomarkers due to water evaporation and loss of samples due to liquid transfer, while giving other advantages including minimizing the matrix effects[25]. Due to the selective nature of this probing method, it is limited to analyte molecules that can form host-guest complexes with CB. It should be noted it is possible to observe interferences from other molecules because CB can bind to different guest molecules. Nevertheless, sample purification such as gel electrophoresis and HPLC can be performed prior to SERS measurement.

The detection scheme demonstrated in this protocol has the potential for multiplexed detection of biomarkers in a complex matrix for clinical applications when it is coupled to advanced data analysis techniques.

ACKNOWLEDGMENTS:

TCL is grateful to the support from the Royal Society Research Grant 2016 R1 (RG150551) and the UCL BEAMS Future Leader Award funded through the Institutional Sponsorship award by the EPSRC (EP/P511262/1). WIKC, TCL and IPP are grateful to the Studentship funded by the A*STAR-UCL Research Attachment Programme through the EPSRC M3S CDT (EP/L015862/1). GD and TJ would like to thank the EPSRC M3S CDT (EP/L015862/1) for sponsoring their studentship. TJ and TCL acknowledge Camtech Innovations for contribution to TJ's studentship. All authors are grateful to the UCL Open Access Fund.

DISCLOSURES:

The authors have nothing to disclose.

REFERENCES:

1. Villa, J. E. L., Poppi, R. J. A portable SERS method for the determination of uric acid using a

paper-based substrate and multivariate curve resolution. *Analyst*. **141** (6), 1966−1972 (2016).
2. Westley, C. et al. Absolute Quantification of Uric Acid in Human Urine Using Surface Enhanced Raman Scattering with the Standard Addition Method. *Analytical Chemistry*. **89** (4), 2472−2477 (2017).
3. Zhao, L., Blackburn, J., Brosseau, C. L. Quantitative Detection of Uric Acid by Electrochemical-Surface Enhanced Raman Spectroscopy Using a Multilayered Au/Ag Substrate. *Analytical Chemistry*. **87** (1), 441−447 (2015).
4. Goodall, B. L., Robinson. A. M., Brosseau, C. L. Electrochemical-surface enhanced Raman spectroscopy (E-SERS) of uric acid: a potential rapid diagnostic method for early preeclampsia detection. *Physical Chemistry Chemical Physics*. **15** (5), 1382−1388 (2013).
5. Lytvyn, Y., Perkins, B. A., Cherney, D. Z. I. Uric Acid as a Biomarker and a Therapeutic Target in Diabetes. *Canadian Journal of Diabetes*. **39** (3), 239−246 (2015).
6. Ali, S. M. U., Ibupoto, Z. H., Kashif, M., Hashim, U., Willander, M. A Potentiometric Indirect Uric Acid Sensor Based on ZnO Nanoflakes and Immobilized Uricase. *Sensors*. **12** (3), 2787−2797 (2012).
7. Yu, J., Wang, S., Ge, L., Ge, S. A novel chemiluminescence paper microfluidic biosensor based on enzymatic reaction for uric acid determination. *Biosensors and Bioelectronics.* **26** (7), 3284−3289 (2011).
8. Yang, Y.-D. Simultaneous determination of creatine, uric acid, creatinine and hippuric acid in urine by high performance liquid chromatography. *Biomedical Chromatography*. **12** (2), 47–49 (1999).
9. Zhao, S., Wang, J., Ye, F., Liu, Y.-M. Determination of uric acid in human urine and serum by capillary electrophoresis with chemiluminescence detection. *Analytical Biochemistry*. **378** (2), 127–131 (2008).
10. Fang, Y., Seong, N.-H., Dlott, D. D. Measurement of the Distribution of Site Enhancements in Surface-Enhanced Raman Scattering. *Science*. **321** (5887), 388−392 (2008).
11. Jeong, H.-H. et al. Dispersion and shape engineered plasmonic nanosensors. *Nature Communications*. **7**, 11331 (2016).
12. Alula, M. T. et al. Preparation of silver nanoparticles coated ZnO/Fe_3O_4 composites using chemical reduction method for sensitive detection of uric acid via surface-enhanced Raman spectroscopy. *Analytica Chimica Acta*. **1073**, 62–71 (2019).
13. Bastús, N. G., Comenge, J., Puntes, V. Kinetically Controlled Seeded Growth Synthesis of Citrate-Stabilized Gold Nanoparticles of up to 200 nm: Size Focusing versus Ostwald Ripening. *Langmuir*. **27** (17), 11098−11105 (2011).
14. Jeong, H.-H. et al. Selectable Nanopattern Arrays for Nanolithographic Imprint and Etch-Mask Applications. *Advanced Science*. **2** (7), 1500016 (2016).
15. Loh, X. J., Lee, T.-C., Dou, Q., Deen, G. R. Utilising inorganic nanocarriers for gene delivery. *Biomaterials Science.* **4** (1), 70−86 (2016).
16. Celiz, A. D., Lee, T.-C., Scherman, O. A. Polymer-Mediated Dispersion of Gold Nanoparticles: Using Supramolecular Moieties on the Periphery. *Advanced Materials.* **21** (38), 3937–3940 (2009).
17. Lee, T.-C., Scherman, O. A. Formation of Dynamic Aggregates in Water by Cucurbit[5]uril Capped with Gold Nanoparticles. *ChemComm.* **46** (14), 2438−2440 (2010).
18. Lee, T.-C., Scherman, O. A. A Facile Synthesis of Dynamic Supramolecular Aggregates of

485 Cucurbit[n]uril (n = 5−8) Capped with Gold Nanoparticles in Aqueous Media. *Chemistry—A*
486 *European Journal***18** (6), 1628−1633 (2012).
487 19. Taylor, R. W. et al. Precise Subnanometer Plasmonic Junctions for SERS within Gold Nano-
488 particle Assemblies Using Cucurbit[n]uril "Glue". *ACS Nano*. **5** (5), 3878−3887 (2011).
489 20. Peveler, W. J. et al. Cucurbituril-mediated quantum dot aggregates formed by aqueous self-
490 assembly for sensing applications. *ChemComm*. **55** (38), 5495−5498 (2019).
491 21. Chio, W.-I. K. et al. Selective Detection of Nitroexplosives Using Molecular Recognition
492 within Self-Assembled Plasmonic Nanojunctions. *The Journal of Physical Chemistry C*. **123** (25),
493 15769−15776 (2019).
494 22. Kasera, S., Biedermann, F., Baumberg, J. J., Scherman, O. A., Mahajan, S. Quantitative SERS
495 Using the Sequestration of Small Molecules Inside Precise Plasmonic Nanoconstructs. *Nano*
496 *Letters.* **12** (11), 5924−5928 (2012).
497 23. Taylor, R. W. et al. In Situ SERS Monitoring of Photochemistry within a Nanojunction
498 Reactor. *Nano Letters.* **13** (12), 5985−5990 (2013).
499 24. Kasera, S., Herrmann, L. O., Barrio, J. d., Baumberg, J. J., Scherman, O. A. Quantitative
500 Multiplexing with Nano-Self-Assemblies in SERS. *Scientific Reports.* **4**, 6785 (2014)
501 25. Chio, W.-I. K. et al. Dual-triggered nanoaggregates of cucurbit[7]uril and gold nanoparticles
502 for multi-spectroscopic quantification of creatinine in urinalysis. *Journal of Materials Chemistry*
503 *C*. **8**, 7051−7058 (2020).
504 26. Turkevich, J., Stevenson, P. C., Hillier, J. A study of the nucleation and growth processes in
505 the synthesis of colloidal gold. *Discussions of the Faraday Society.* **11**, 55−75 (1951).
506 27. Lagona, J., Mukhopadhyay, P., Chakrabarti, S., Issacs, L. The cucurbit[n]uril family.
507 *Angewandte Chemie International Edition.* **44** (31), 4844−4870 (2005).
508 28. OceanView Installation and Operation Manual.
509 https://www.oceaninsight.com/globalassets/catalog-blocks-and-images/manuals--instruction-
510 old-logo/software/oceanviewio.pdf (2013).
511 29. Mahajan, S. et al. Raman and SERS spectroscopy of cucurbit[n]urils. *Physical Chemistry*
512 *Chemical Physics*. **12** (35), 10429−10433 (2010).
513 30. Langer, J. et al. Present and Future of Surface-Enhanced Raman Scattering. *ACS Nano*. **14**
514 (1), 28−117 (2020).
515 31. Pilot, R. et al. A Review on Surface-Enhanced Raman Scattering. *Biosensors*. **9** (2), 57 (2019).
516 32. Bantz, K. C. et al. Recent progress in SERS biosensing. *Physical Chemistry Chemical Physics*.
517 **13** (24), 11551−11567 (2011).
518 33. Moore, T. J. et al. In Vitro and In Vivo SERS Biosensing for Disease Diagnosis. *Biosensors*. **8**
519 (2), 46 (2018).
520 34. Bonifacio, A., Cervo, S., Sergo, V. Label-free surface-enhanced Raman spectroscopy of
521 biofluids: fundamental aspects and diagnostic applications. *Analytical and Bioanalytical*
522 *Chemistry*. **407** (27), 8265−8277 (2015).
523 35. Jeong, H.-H., Choi, E., Ellis, E., Lee, T.-C. Recent advances in gold nanoparticles for
524 biomedical applications: from hybrid structures to multi-functionality. *Journal of Materials*
525 *Chemistry B*. **7** (22), 3480−3496 (2019).
526 36. Premasiri, W. R., Clarke, R. H., Womble, M. E. Urine Analysis by Laser Raman Spectroscopy.
527 *Lasers in Surgery and Medicine*. **28**(4), 330−334 (2001).
528 37. Lu, Y. et al. Superhydrophobic silver film as a SERS substrate for the detection of uric acid

and creatinine. *Biomedical Optics Express*. **9** (10), 4988−4997 (2018).
38. Feig, D. I. et al. Serum Uric Acid: A Risk Factor and a Target for Treatment? *Journal of the American Society of Nephrology*. **17** (4), 69−73 (2006).
39. Maiuolo, J., Oppedisano, F., Gratteri, S., Muscoli, C., Mollace, V. Regulation of uric acid metabolism and excretion. *International Journal of Cardiology*. **213**, 8−14 (2016).

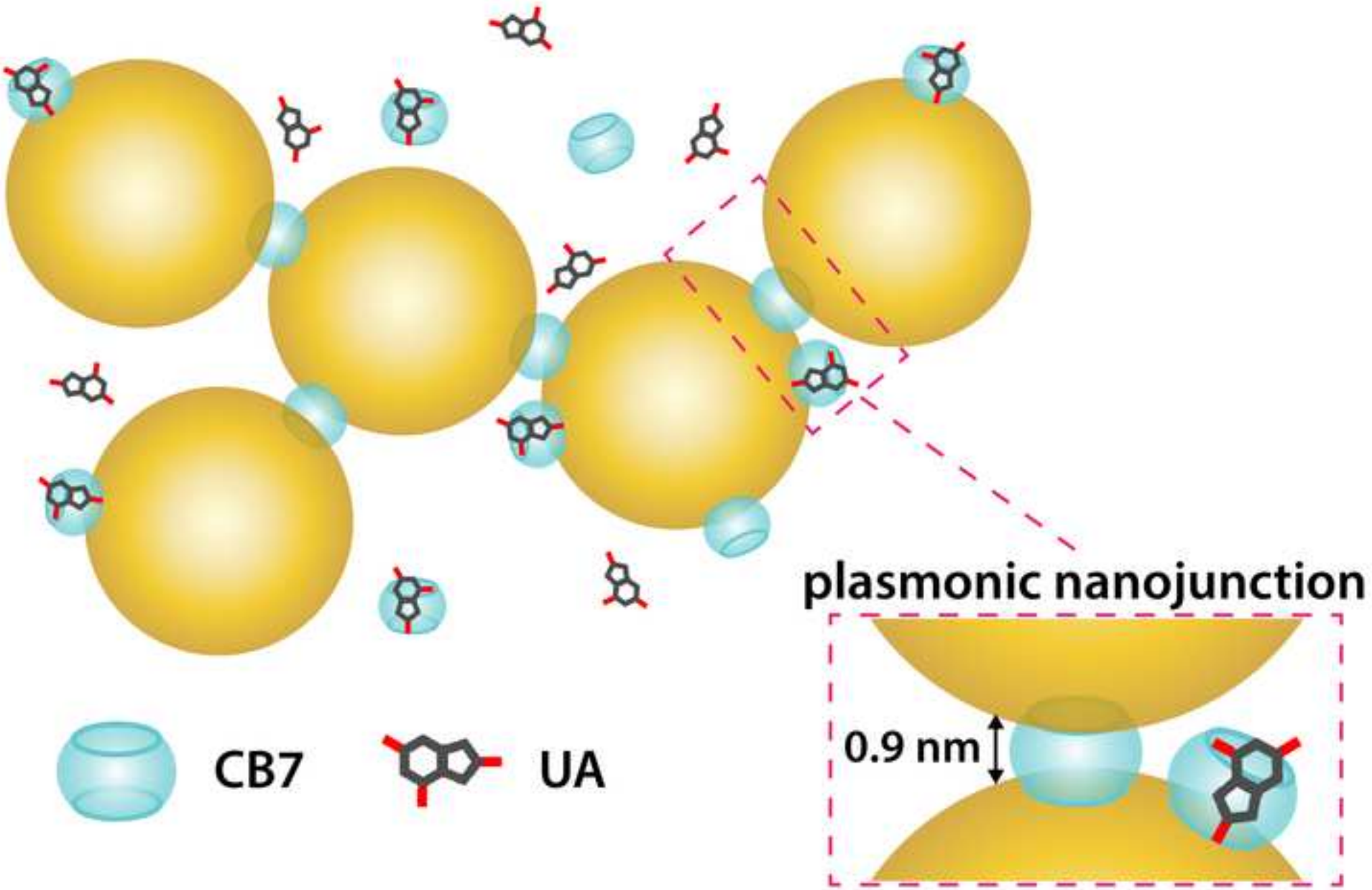

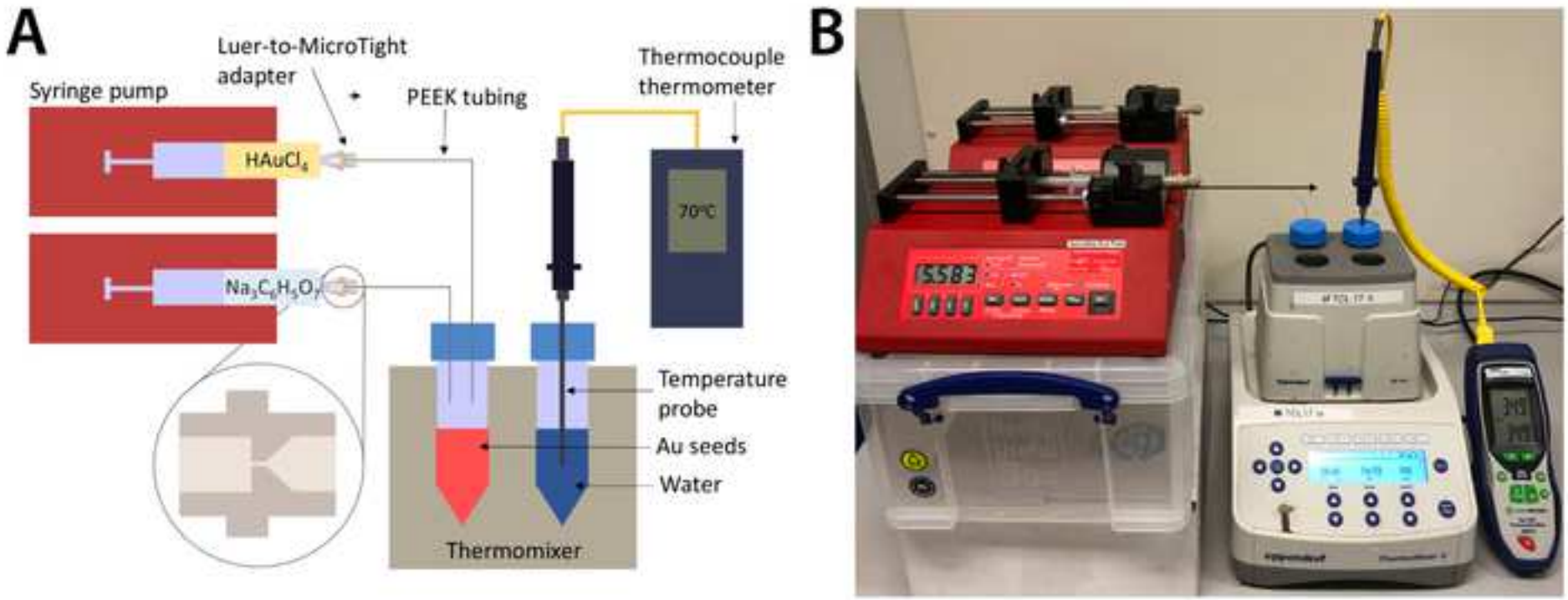

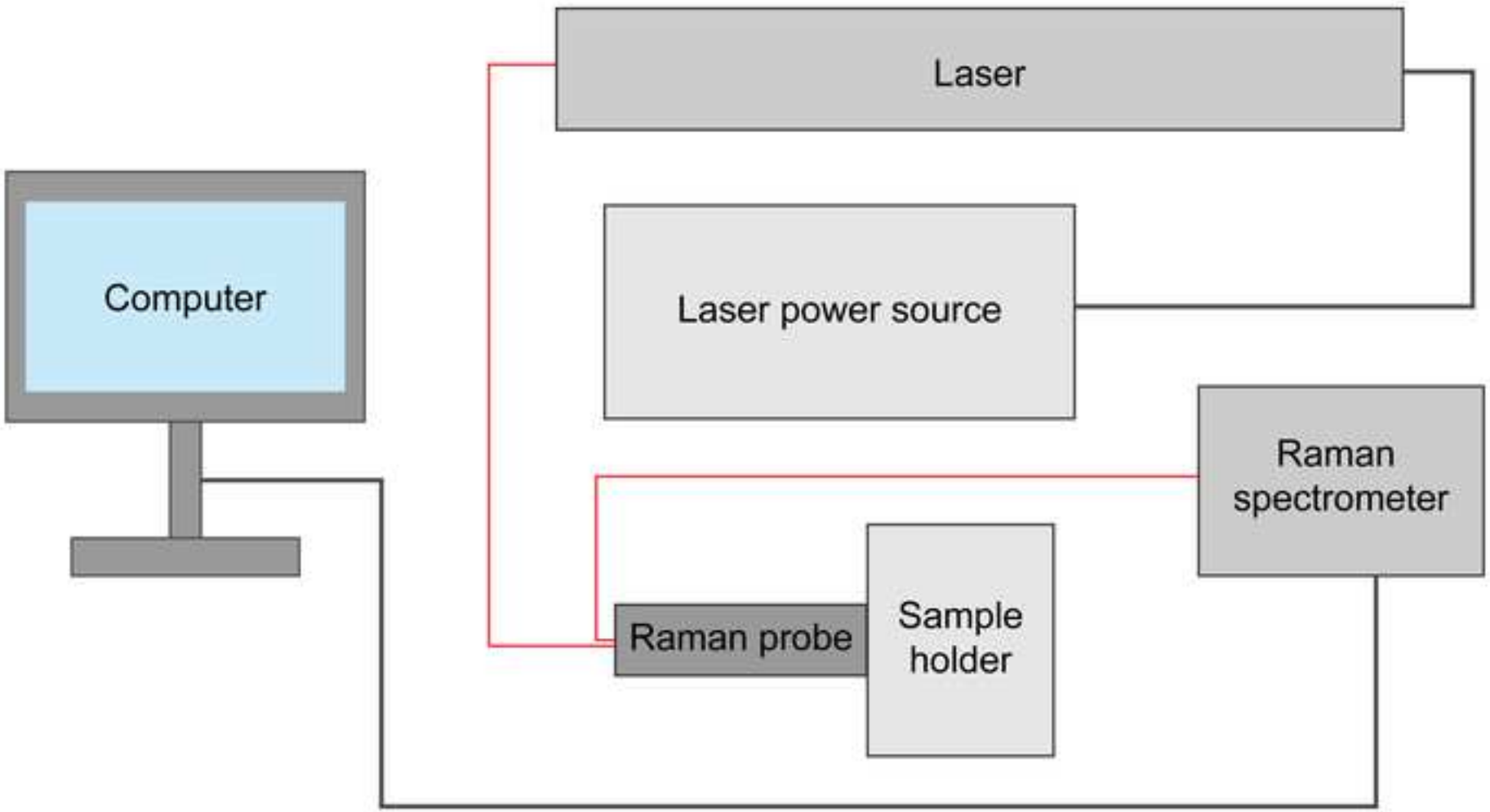

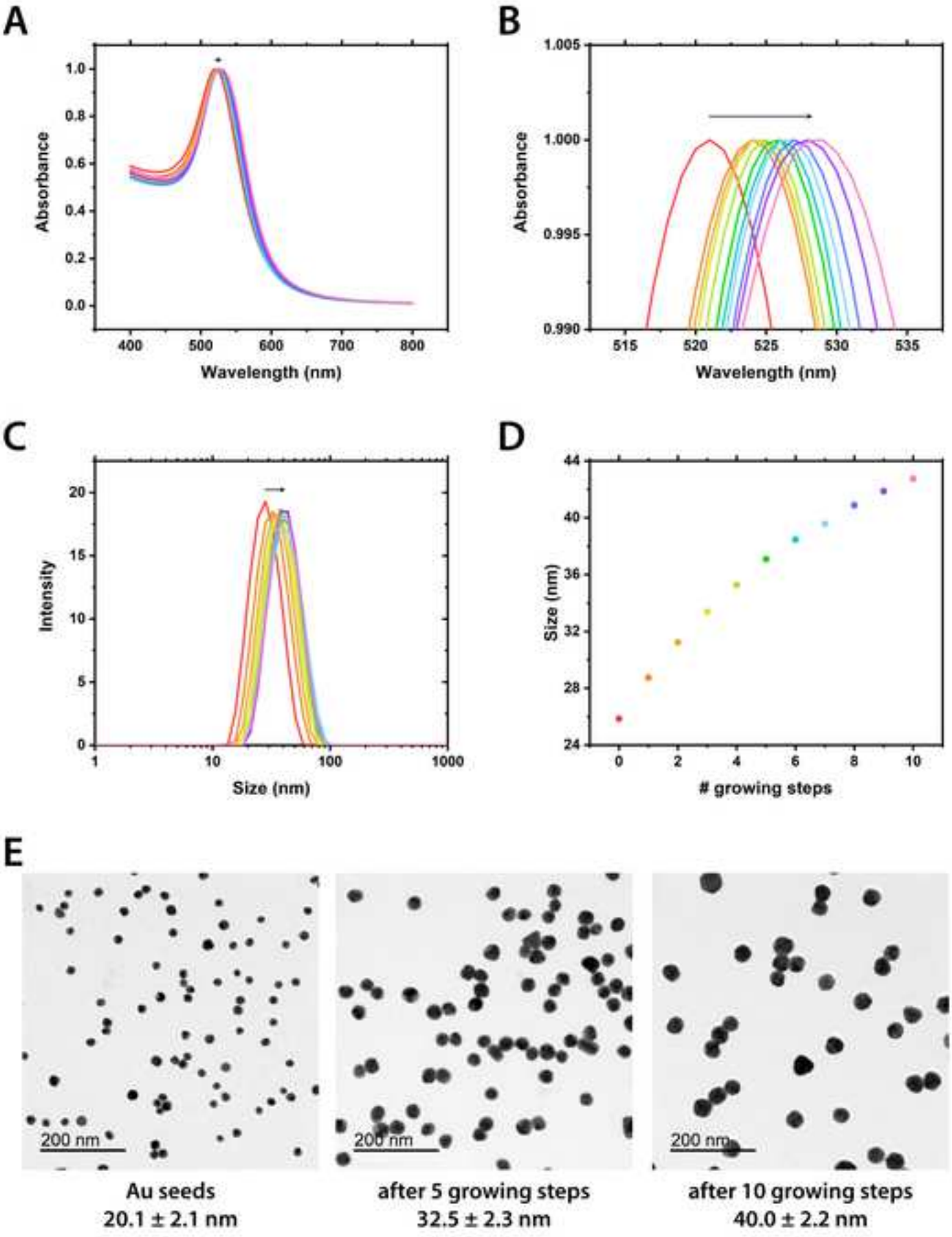

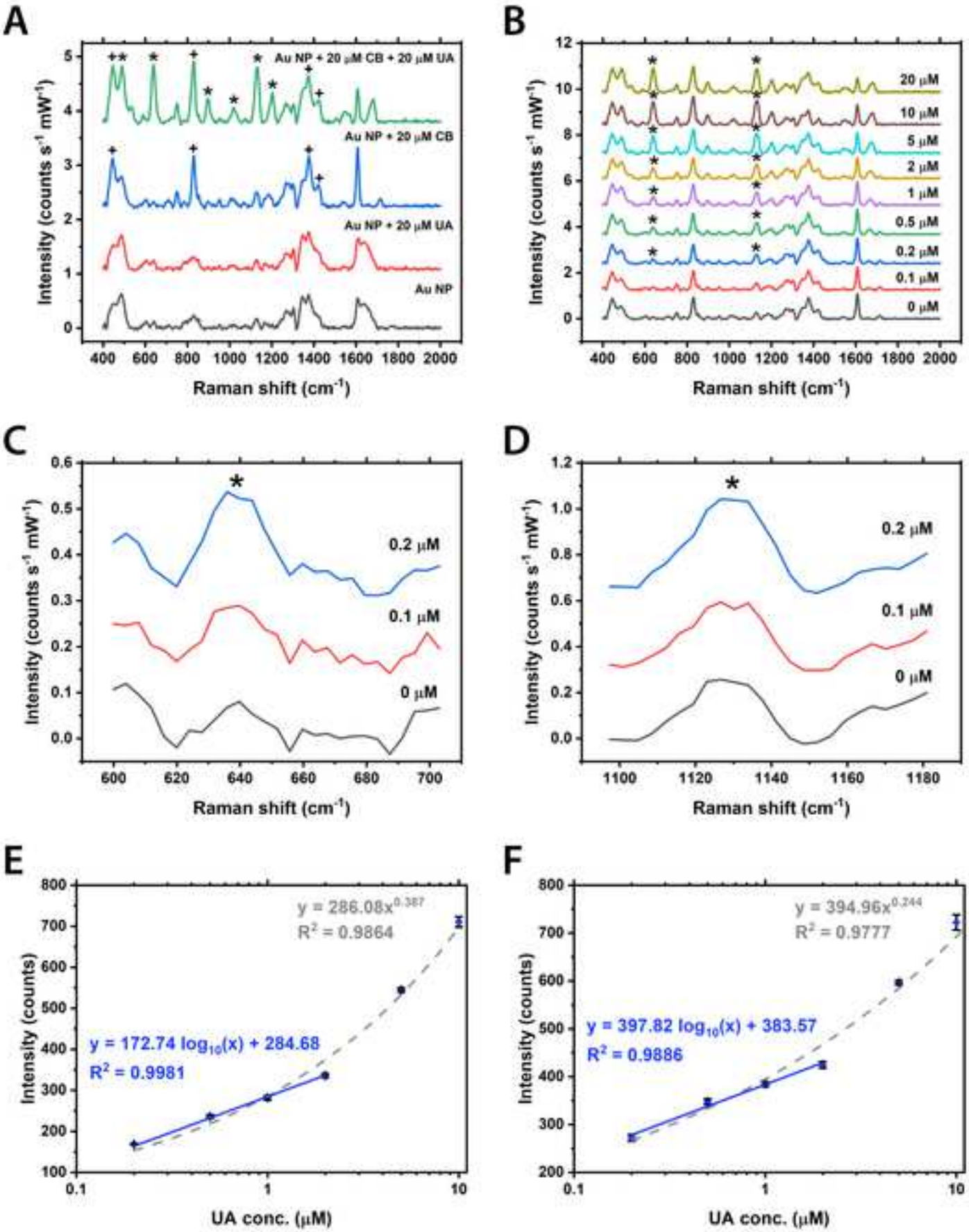

Conc. of UA stock solution (μM)	Vol. of UA stock solution added (mL)	Vol. of water added (mL)
400	5	5
200	5	5
100	4	6
40	5	5
20	5	5
10	4	6
4	5	5

Conc. of new UA stock solution (µM)
200
100
40
20
10
4
2

CB7		UA
SERS peak (cm^{-1})	Peak assignment	SERS peak (cm^{-1})
446	Ring scissor mode	491
831	Ring deformation	640
1375	Symmetric C-N stretching	896
1420	Asymmetric C-N stretching	1020
		1130
		1202

Peak assignment
C-N-C ring vibration
Skeletal ring deformation
N-H bending
Ring vibration
C-N vibration
N-C-C stretching and bending

Name of Material/ Equipment	Company	Catalog Number
40 nm gold nanoparticles	NanoComposix	AUCN40-100M
Centrifuge tube	Corning Falcon	14-432-22
Cucurbit[7]uril	Lab-made	
Gold(III) chloride trihydrate	Sigma aldrich	520918
Luer lock disposable syringe	Cole-Parmer	WZ-07945-15
Luer-to-MicroTight adapter	LuerTight	P-662
PEEK tubing	IDEX	1572
PEEK tubing cutter	IDEX	WZ-02013-30
Raman spectrometer	Ocean Optics	QE pro
Sodium citrate tribasic dihydrate	Sigma aldrich	S4641
Sonicator		
Standard Probe	Digi-Sense	WZ-08516-55
Syringe pump	Aladdin	ALADDIN2-220
Thermocouple thermometer	Digi-Sense	WZ-20250-91
ThermoMixer	Eppendorf	5382000031
Uric acid	Sigma aldrich	U2625

	Comments/Description
	NanoXact, 0.05 mg/ mL, bare (citrate)
	50 mL volume
	see ref. 19
	≥99.9% trace metals basis
	3 mL volume
	360 µm outer diameter Tubing to Luer Syringe
	360 µm outer diameter, 150 µm inner diameter
	Capillary Polymer Chromatography Tubing Cutter For 360 µm to 1/32" OD tubing
	ACS reagent, ≥99.0%
	Type-K
	2 syringes, maximum syringe volume 60 mL
	Single-Input Thermocouple Thermometer with NIST-Traceable Calibration
	With an Eppendorf SmartBlock for 50 mL tubes
	≥99%, crystalline

Editorial comments:

Please take this opportunity to thoroughly proofread the manuscript to ensure that there are no spelling or grammar issues. The JoVE editor will not copy-edit your manuscript and any errors in the submitted revision may be present in the published version.

Author reply: We thank the editor for assessing our manuscript and we have proofread our manuscript thoroughly.

Reviewers' comments:
Reviewer #1:

Authors revised the manuscript partly.

Author reply: We thank the reviewer for assessing our manuscript.

The assignment for the Raman peaks is absent.

Response: We have already addressed the reviewer's comments in the previous version of the manuscript (see Table 2) and the previous rebuttal letter.

The possible interfering species should be checked.

Response: CB and citrate are the only species in the sample apart from Au NPs and UA. By comparing the SERS spectra of Au NP + CB + UA and Au NP + CB in Figure 5A, CB and citrate do not show any notable impact on the SERS signals of UA, as validated by the observed monotonic correlation between SERS intensity and concentration of UA. This point had already been discussed in the existing main text (Page 10, paragraph 1).

Reviewer #3:

The manuscript entitled 'Quantitative SERS Detection of Uric Acid via Formation of Precise Plasmonic Nanojunctions within Aggregates of Gold Nanoparticles and Cucurbit[n]uril' reports on the generation of gold nanoparticles and describes a rapid and sensitive method for the quantitative detection of uric acid (UA), via surface enhanced Raman spectroscopy. The manuscript is well-written and organised.

Author reply: We thank the reviewer for assessing our manuscript and are grateful that they found our manuscript well-written and organised. We have made the changes to the manuscript in response to the reviewer's comments. The text added is marked in green.

It would be better to give more explanation regarding the control of aggregation.

Response: (Page 9) We have added "via carbonyl portal binding".

(Page 10) We have added "The aggregation of Au NPs mediated by CB7 in our experimental setting is expected to follow the diffusion-limited colloidal aggregation (DLCA) kinetics[19], in which open and elongated chain-like structures were rapidly formed initially before joining together as quasi-fractal network. DLCA kinetics typically occurs at a high CB: Au NP ratio (by number), which is equal to 10^6:1 in our case."

Reviewer #4:

This manuscript describes a simple method of preparation of AuNPs for SERS measurement of uric acid. The methods are written nicely and clearly. We advise the authors to consider the following issues before it is accepted for publication.

Author reply: We thank the reviewer for assessing our manuscript and are grateful that they found our methods written nicely and clearly. We have made the changes to the manuscript in response to the reviewer's comments. The text removed is indicated in ~~blue and struck through~~, while the text added is marked in green.

The authors should state the advantages of their method with the already available methods in the literatures in the introduction part. The following citation may help the author (Analytica Chimica Acta, 1073, 2019, 62-71)

Response: (Page 2) We have replaced "~~complex metal nanostructures and are widely used in biomedical applications owing to their superior properties[12-15]~~" by "the time-consuming fabrication of complex metal nanocomposites[12], and thus are widely used in biomedical applications owing to their superior properties[13-16]" and cited the suggested reference.

The selectivity of the method is not done. Authors should show the performance of their new method in detecting of potential interfering molecules like creatinine, urea, and some amino acids.

Response: This detection scheme is known to selectively enhance the signals from analyte molecules that can form host-guest complexes with CBs, which has been illustrated in our recent study of creatinine in synthetic urine (ref. 25) and our previous work on detection of explosive markers (ref. 21). It is possible to identify the potential interfering molecules that also bind to CB by their characteristic SERS signals. Multiplexed detection of the potential interfering molecules could be interesting and has been demonstrated in our previous study on nitroaromatics (ref. 21) but beyond the scope of this methodology manuscript.

The feasibility of the method in detection of uric acid in real samples like urine, blood are not demonstrated.

Response: We have suggested this as a potential application, as illustrated in our recent study of creatinine in synthetic urine (ref. 25) and work by others (ref. 24). The methodology for sample preparation and SERS detection of UA in real samples should be the same as the protocol described in this manuscript, while additional data analysis techniques would be required. This point has been discussed in the existing main text (page 10, paragraph 2). The

application in real samples is an interesting topic but beyond the scope of this methodology manuscript.

How about the enhancement factor?

Response: The UA signals cannot be detected at its saturated concentration in our experimental setting. Therefore, enhancement factor, EF = $(I_{SERS}/N_{SERS})/(I_{RS}/N_{RS})$ where I_{RS} is normalised Raman signal intensity of UA, cannot be estimated accurately.

Gemma Davison received her MPhys in Experimental Physics from the University of York in 2018. She is currently studying for a PhD at University College London under the supervision of Dr Tung-Chun Lee. Her research interests include the synthesis of hybrid nanoparticles for applications in solar energy and PIERS sensing.

Jia Liu received MSc degree in Advanced Materials Science from University College London in 2018. She is currently studying for a PhD in Chemistry of University College London under the supervision of Dr. Tung-Chun Lee. Her research interests include the host-guest systems, electrochemistry-based sensing and electrochemical surface-enhanced Raman spectroscopy (EC-SERS).

Dr. Tung-Chun Lee received his BSc in Chemistry from University of Hong Kong in 2005 and his PhD in Chemistry from University of Cambridge in 2012. He was a Post-doctoral Fellow at the Max Planck Institute for Intelligent Systems from 2011 to 2014 before he joined the University College London as a Lecturer and started his independent academic career. His research interests include exotic nanoparticles, nanofabrication, nanochemistry, active matter and supramolecular chemistry. Currently, he is leading an interdisciplinary group of 11 researchers exploring chemistry under nano-confinement, active propulsion at the nanoscale and metamaterial sensors.

Tabitha Jones received her MEng in Materials Science from the University of Oxford in 2017. She is currently studying for an EngD at University College London under the supervision of Dr. Tung-Chun Lee. Her research interests include plasmonic nanostructures, biosensors and electrochemical surface-enhanced Raman spectroscopy (EC-SERS).

Weng-I Katherine Chio received her BEng Materials Science and Engineering and MRes Nanomaterials from Imperial College London in 2015 and 2016 respectively. She is currently studying for a PhD at University College London under the supervision of Dr. Tung-Chun Lee and Prof. Ivan P. Parkin, with a two-year research attachment at Singapore Bioimaging Consortium (SBIC), Agency for Science, Technology and Research (A*STAR) under the supervision of Prof. Malini Olivo. Her research interests include nanomaterials, supramolecular chemistry and surface-enhanced Raman spectroscopy for sensing applications.